Preliminary phantom-based dynamic calibration techniques assessment for microwave colonoscopy systems

Alejandra Garrido-Atienza*†, Walid Dghoughi *, Jordi Romeu Robert†, Marta Guardiola Garcia*
*MiWEndo Solutions: Barcelona, Spain, agarrido@miwendo.com
†Universitat Politècnica de Catalunya: Barcelona, Spain

***Abstract*—Early detection and resection of colon polyp is the best way to reduce colorectal cancer (CRC) mortality. The current method for early detection is colonoscopy, which has a limited field of view, and its efficacy is highly dependant on the endoscopist's experience and colon preparation. This work presents a device for combining microwave imaging with optical colonoscopy. The challenges of this new microwave imaging system are presented, such as the unknown distance to the colon mucosa, which leads to undesired scattered fields and, the antenna size limitations. Four dynamic calibration techniques are proposed to remove the effects of the undefined distance from the imaging region to colon mucosa. These calibration methods are based on averaging the colonoscopy trajectory frames and subtracting the calibration set from the current frame. The phantom preliminary results show that these calibration methods completely delete the undesired scatter.**

***Index Terms*—endoscopes, medical diagnostic imaging, microwave antenna arrays, microwave imaging, back-propagation algorithms.**

I. Introduction

Microwave imaging is widely used in different applications such as non-destructive testing [1] and medical diagnostics and treatment. In the case of medical imaging, a clear example is breast cancer detection, where there are multiple benefits of using microwave imaging in terms of cost, patient's comfort, and safety when compared to current mammography techniques [2]. A more recent application of microwave imaging is colorectal cancer (CRC) early detection [3]. The CRC is the second most common cause of cancer death in both women and men. Usually, the CRC cases start as a growth of tissue, called a polyp, which commonly appears in patients over 50 years. Some kinds of polyps, known as adenomas, are the precursors of the 90% of CRC cases [4]. For this reason, polyp detection and resection are crucial to reducing mortality. The gold standard for early detection of CRC and most effective method for diagnosing and removing polpyps throughout the colon is optical colonoscopy. Nevertheless, due to the limited field of view of the camera (less than 180º), poor colon preparation, and the varying endoscopist's experience, there is a polyp miss rate of 22% [5] and the risk of developing CRC after a negative colonoscopy is 8% [6].

This paper reports a device for combining microwave imaging with optical colonoscopy as an accessory adjustable at the distal end of a standard colonoscope. A colonoscope is a flexible tube 1.5 m with an optical camera 14 mm at its distal end. The colonoscope is introduced into the patient's colon, a tubular organ. With the suggested system, the detection of polyps can be automatized by sounding an alarm when a polyp is detected to warn the endoscopist. The proposed microwave colonoscopy system has multiple advantages compared to the standard optical colonoscopy: (i) It increases the field of view up to 360º, (ii) Detection is automatic and independent from the endoscopist's experience, and (iii) It provides new data based on dielectric properties, which are sensitive and specific to colon polyps [7]. Microwave imaging applied to endoscopy is very different than previously studied applications of medical microwave imaging. As a benefit, there is no requirement to penetrate the tissues, as polyps are on the surface of the colon. Nevertheless, challenges appear; for example, the number of antennas is limited due to size constraints of the device. Also, each antenna dimension must be reduced, leading to an increase in mutual coupling. Due to the size limitations, the antennas must be electrically small, limiting the bandwidth and hence allowing only frequency-domain imaging algorithms. Usually, the antennas are distributed surrounding the imaging region, but in this endoscopic scenario the imaging region encloses the circular array. The last and most crucial challenge is that the distance from the imaging region to the antenna is unknown and constantly changes. Hence, calibration techniques must be investigated to remove this uncertainty from the measured scattered fields.

II. Microwave colonoscopy system

The imaging system is composed of a processing unit and an acquisition system. The acquisition system goal is to illuminate the object under test, the colon, with incident radiation, E^i, and measure the total received fields, E^t, resulting from the interaction of the incident radiation and the body under test. The data collected is sent to the processing unit to reconstruct an image of the dielectric properties' profile of the object under test. This reconstruction process is based on the fact that the E^t is the superposition of the E^i and the scattered field, E^s, which contains the spatial changes information of the dielectric properties of the phantom. This system is designed to be attached at the tip of a conventional colonoscope, and it will measure during the whole colonoscopy exploration. At

 http://dx.doi.org/10.23919/EuCAP53622.2022.9769259

the same time, the processing unit analyzes the measurements and emits an alarm when a polyp is detected.

A. Acquisition system

The acquisition system is formed by a cylindrical ring-shaped accessory containing two switched arrays of eight antennas organized in two rings. One ring includes the transmitting antennas and the other the receiving antennas. The antennas are cavity-backed slot antennas fed by microstrip lines as described in [3]. The final dimensions of the acquisition device are 20 mm in diameter by 30 mm in length, having a total thickness of 3 mm. The antennas are designed to operate in the air over the 7.6-7.66 GHz. The reduced bandwidth is due to the miniaturization of the antennas.

B. Processing unit

The processing unit is aimed to generate, receive and process the microwave signals, and as a result, emits an alarm when a polyp is detected. The processing algorithm is composed of three steps repeated for each frame. Each frame contains the information of a cross-section of the colon, and consists of a vector of 24 S21 parameters at 7.6 GHz obtained with a standard Vector Network Analyzer (VNA) by alternately selecting the three closest receiving antennas for each transmitting antenna, i.e. the directly adjacent antenna and the two diagonally adjacent ones. The three steps performed by the processing unit for each frame are the following: (i) Cleaner: the calibration removes from E^t the unwanted effects other than the target, i.e., the polyp. This includes the callenges of dealing with the unknown distance from the healthy colon walls, the colon folds, and angulations, etc. (ii) Focuser: once data are calibrated, it is focused, using the Modified Monofocusing algorithm [8]:

$$I_{z_i}(\vec{r}) = \left| \sum_{k=(j-1)N_a}^{(j+1)N_a} \sum_{j=1}^{N_a} E_s^2(r_{\vec{T}_j}, r_{\vec{R}_k}, z_i) \right. \\ \left. J_1^2(k|r_{\vec{R}_k} - \vec{r}|) e^{j2(k|r_{\vec{R}_k} - \vec{r}| + \varphi)} \right| \quad (1)$$

Being $k = 2\pi cf$ the wavenumber and φ the angle between the transmitting and the receiving antennas. This Focuser method provides the image of the dielectric contrast profile $I_{z_i}(\vec{r})$; (iii) Detector: for each reconstructed image frame $I_{z_i}(\vec{r})$, the thresholding method compares the maximum of the current reconstruction with the average most of the previous reconstructed images from the frames classified as healthy and used for the calibration, $I_{z_{h,j}}(\vec{r})$ as:

$$\frac{max(Iz_i(\vec{r}))}{\sum_{j=1}^{N_h} \frac{1}{N_h} max(I_{z_{h,j}}(\vec{r}))} > Th \quad (2)$$

Where Th is the contrast threshold that allows deciding whether it is a polyp or not, N_h is the number of healthy frames used to calibrate the current frame i and, I_{z_i} and $I_{z_{h,j}}$ the reconstructed image of the current frame and each healthy frame respectively.

C. Measurement setup

To model a colon during a colonoscopy, we have built a phantom with the dielectric properties of an inflated human colon. We modeled the segmented appearance of the colon (colon folds) by making slits in the polystyrene cylinder every 45 mm. The phantom is composed of a cylinder of expanded polystyrene modeling the colon lumen of dimensions 268 mm length by 66.7 mm diameter as presented in Fig. 1. The lumen model is positioned in a cylindrical container of 300 mm length by 150 mm diameter made of methacrylate.

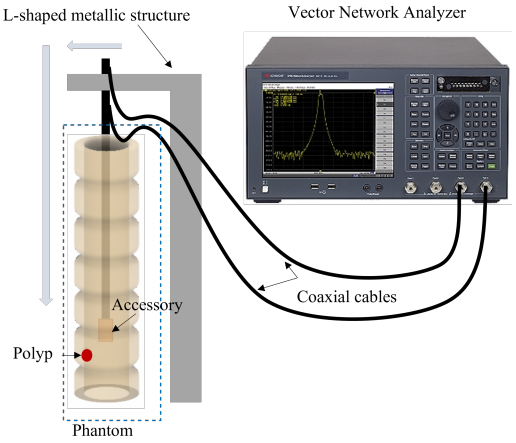

Fig. 1. Phantom measurement setup

The container is filled with an oil-gelatin-based material that mimics the dielectric properties of healthy colon mucosa based on a recipe developed for breast phantoms [9]. The polyp is a 10 mm sphere made of a similar material but with the dielectric properties of an adenocarcinoma [7][10].

To be able to reproduce a realistic colonoscopy exploration [11] inside the phantom, we have built a 3D positioning system [10] composed of an L-shaped metallic structure on top of a plastic base that supports a plastic bar equipped with a ruler to move the accessory along the z-direction. The phantom is placed on mobile supports to be carried in the XY plane.

III. Calibration techniques

This section presents four different techniques to remove the undesired scattered signals in real-time applications. The main effect to be removed is the device's movement and the colon, which results in the colon wall being at unknown and varying distances. Ideally, to isolate the target, the scattered field measured in the corresponding "healthy" scenario must be subtracted to E^t. By the "healthy" scenario, we mean the same scenario but without the polyp, which is not available in clinical practice. Because of this, we have developed several strategies to emulate this ideal calibration by taking advantage of having continuous measurement frames of the colon that are very similar to each other and the fact that the vast majority of the colon mucosa is healthy and polyps appear isolated.

A. Healthy Average Temporal (HAT) subtraction

This method consists of subtracting the average of the healthy steps of the trajectory to each step, as shown in 3.

$$E^s_{z_i,HAT}(\vec{r},f) = E^t_{z_i}(\vec{r},f) - \sum_{j=1}^{N_h} \frac{1}{N_h} E^t_{z_{h,j}}(\vec{r},f) \quad (3)$$

Where N_h is the number of healthy steps averaged. This approach is also unrealistic because it assumes a knowledge of which frames are healthy. However, it is feasible in a phantom study where the trajectory is well-characterized.

B. Total Average Temporal (TAT) subtraction

As mentioned before, in general, most of the parts of the colon are healthy. Based on this, we have developed the Total Average Temporal subtraction (TAT), where the calibration set for a current frame i is the average of all prior frames, as shown in 4, with the hypothesis that the average set obtained will model the healthy colon accurately.

$$E^s_{z_i,TAT}(\vec{r},f) = E^t_{z_i}(\vec{r},f) - \sum_{j=1}^{N_p} \frac{1}{N_p} E^t_{z_j}(\vec{r},f) \quad (4)$$

Where N_p is the number of frames, there are before the current frame i.

C. Hop and N Average Temporal (HNAT) subtraction

Another technique, designed to avoid averaging polyp frames, is the Hop and N Average Temporal (HNAT) subtraction. The idea is to skip H frames which could contain polyp, and average the N prior frames, as formulated in 5. The performance of this technique depends on the definition of H. If H is too large, then the frames used to calibrate are too different from the current frame; thus, it cannot accurately model the current colon section. Also, H depends on the polyp size, which is unknown.

$$E^s_{z_i,HNAT}(\vec{r},f) = E^t_{z_i}(\vec{r},f) - \sum_{j=i-N-H}^{i-H} \frac{1}{N} E^t_{z_j}(\vec{r},f) \quad (5)$$

In 5, N is the number of frames averaged, and the H is the number of previous frames to the current one we skipped for the calibration.

D. Adaptive N Average Temporal (ANAT) subtraction

Finally, the last technique tested with the phantom is an upgraded version of HNAT but avoids H. This method uses the detection information from the previous frame: if the last frame is detected as a polyp, then it is not taken into account for the average, whereas if the previous frame is considered healthy, it is used in the calibration.

$$E^s_{z_i,ANAT}(\vec{r},f) = E^t_{z_i}(\vec{r},f) - \sum_{j=i-Nnp-1}^{Nnp} E^t_{z_j}(\vec{r},f) \quad (6)$$

Where N_{np} is the number of prior frames of the current frame i that have not been detected as a polyp.

IV. Phantom validation results

To analyze the calibrations proposed above, we have measured a non-uniform trajectory varying in YZ plane, of 260 mm in length with a distance between frames of 4 mm. A polyp of 10 mm in diameter is located between frames 45 and 48. The non-uniform trajectory is presented in Fig. 2, the idea of this trajectory is to evaluate if the algorithm can distinguish between a movement towards the colon wall whether there is a polyp or not. It is possible to see a movement towards the colon mucosa without polyp around z = 88 mm and another towards the polyp.

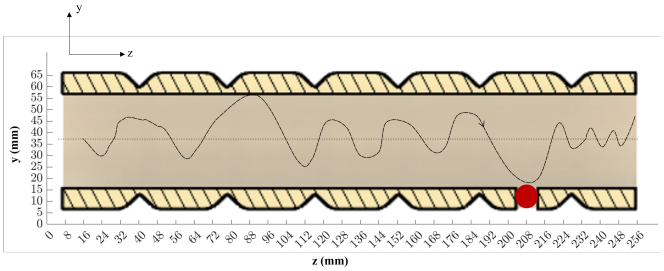

Fig. 2. Device trajectory along the phantom.

Fig. 3 represents in the left y-axis the variation of position the y of the accessory inside the colon model. The right axis shows the evolution of the dielectric contrast reconstruction along the trajectory. We select the maximum of the dielectric contrast reconstruction for each frame, which corresponds to the pixel with higher dielectric contrast. It is known that the polyp is between frames 45 and 48, so this region must have higher contrast than in the other regions. The red diamonds indicate that there is a positive detection.

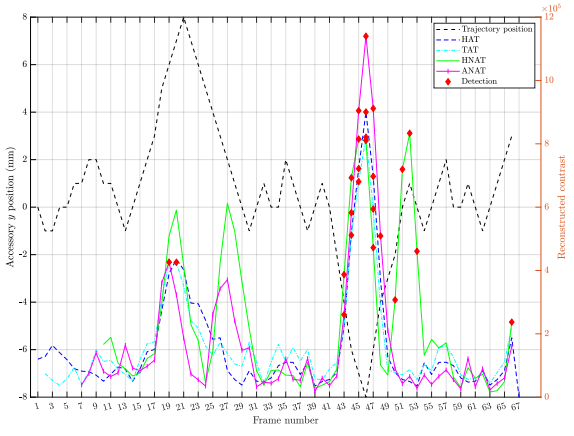

Fig. 3. Maximum contrast reconstructed for each frame of the trajectory for the calibrations:(i) HAT in dark blue; (ii) TAT in cyan; (iii) HNAT in green; (iv) ANAT in magenta.

As expected when using the HAT calibration, the polyp region is perfectly detected. Comparing the TAT calibration with the HAT, it is possible to observe that the detection

also happens inside the polyp region. Still, two false positives in frames 19 and 20 have appeared. Those false positives, corresponding to the region with elevated accessory movement (see trajectory line), are caused because the frames used for calibration (frames from 1 to 18) have lower displacement than in this region, and these frames cannot compensate the movement accurately.

On the other hand, the HNAT calibration for $H = 3$ (meaning the number of skipped frames is three) and $N = 6$ (the number of frames to average the healthy colon correctly taking into account the accessory movement), the goal is to skip the polyp to avoid false positives after it. Still, there is a false positive detection of three frames after the polyp region because those frames are calibrated with polyp frames. This behavior is natural as the frames after the polyp are still calibrated with some unhealthy frames. This effect can be avoided by increasing N to have more healthy frames than polyp in the averaging signal or automatically eliminating the polyp frames from the calibration set. This second option is the last strategy tested, the ANAT calibration ($N = 6$ maintaining the same value as HNAT calibration). It is possible to see in Fig. 3 that the ANAT method is the one that suits better with the HAT. This technique gives good contrast in the healthy region, calibrates the movement accurately, and avoids false positives after the polyp because the positive frames are not used in the calibration even though this strategy is highly dependant on the detection strategy, which is still under development.

V. Conclusions and Future work

This paper presents an algorithm for microwave colonoscopy that we validated with phantoms. The main challenge is to find the best calibration method for the novel microwave colonoscopy system. The TAT was an excellent first version for long and stable trajectories, which have more healthy frames than polyp ones, but it does not calibrate precisely the accessory movement. The HAT calibration allows polyp detection and correctly eliminates the scattering of the the region with abrupt accessory movement. However, multiple false positives appear after the polyp region (frames 50, 53, and 66). The results obtained reflect that the ANAT calibration is the one that reproduces better the results of the ideal calibration (HAT) and correctly removes the effects of the accessory movement. The result achieved is for a calibration using $N = 6$; this parameter is still under study to be fully defined. Moreover, the performance of ANAT calibration depends on the threshold technique used for the detector. Future ideas to improve the calibration are related to using metrics to compare the similarity between frames and choose which one suits better to calibrate them. To improve the detector, we are studying outlier detection methods. Finally, the calibration technique must be validated with more trajectories and realistic phantoms. Preliminary validation with phantoms shows the feasibility of using microwave colonoscopy for colon polyp detection.

Acknowledgment

A.G. acknowledges the financial support from DIN2019-010857, M.G., and W.D acknowledge the financial support from the European Union's Horizon 2020 research and innovation programme under grant agreement No 960251 and from the European Institute of Innovation and Technology (EIT). J.R. acknowledges the financial support from Agencia Estatal Investigación PID2019-107885GB-C31/AEI/10.13039/.

References

[1] H. Alidoustaghdam and M. Çayören, *"Non-Destructive Testing of Concrete Tunnels With Qualitative Microwave Imaging,"* 2020 German Microwave Conference (GeMiC), 2020, pp. 29-31.

[2] M. Elsdon, M. Leach, M. J. Fdo, S. J. Foti and D. Smith, *"Early Stage Breast Cancer Detection using Indirect Microwave Holography,"* 2006 European Microwave Conference, 2006, pp. 1256-1259, doi: 10.1109/EUMC.2006.281223.

[3] M. Guardiola et al., *"Design and evaluation of an antenna applicator for a microwave colonoscopy system,"* IEEE Trans. Antennas Propag., vol. 67, no. 8, 2019.

[4] R. L. Siegel, K. D. Miller, and A. Jemal, *"Cancer statistics, 2015,"* CA. Cancer J. Clin., vol. 65, no. 1, pp. 5–29, 2015.

[5] J. C. van Rijn, J. B. Reitsma, J. Stoker, P. M. Bossuyt, S. J. van Deventer, and E. Dekker, *"Polyp miss rate determined by tandem colonoscopy: a systematic review,"* Am J Gastroenterol, vol. 101, no. 2, pp. 343–350, 2006.

[6] N. J. Samadder et al., *"Characteristics of missed or interval colorectal cancer and patient survival: a population-based study,"* Gastroenterology, vol. 146, no. 4, pp. 950–960, 2014.

[7] Guardiola M, Buitrago S, Fernández-Esparrach G, O'Callaghan JM, Romeu J, Cuatrecasas M, Córdova H, González Ballester MÁ, Camara O. *"Dielectric properties of colon polyps, cancer, and normal mucosa: Ex vivo measurements from 0.5 to 20 GHz."* Med Phys. 2018 May 28.

[8] A. Zamani and A. Abbosh, *"Hybrid Clutter Rejection Technique for Improved Microwave Head Imaging,"* in IEEE Transactions on Antennas and Propagation, vol. 63, no. 11, pp. 4921-4931, Nov. 2015, doi: 10.1109/TAP.2015.2479238.

[9] M. G. Di Meo S, Pasotti L, Iliopoulos I, Pasian M, Ettorre M, Zhadobov M, *"Tissue-mimicking materials for breast phantoms up to 50 GHz,"* Phys Med Biol., vol. 5, no. 64, 2019.

[10] Garrido A, Sont R, Dghoughi W, Marcoval S, Romeu J, Fernández-Esparrach G, et al. *"Polyp Automatic Detection using Microwave Endoscopy for Colorectal Cancer Prevention and Early Detection. Phantom Validation."* IEEE Access *(under review)*

[11] K. G. V. Jagadeesan Jayender, Raul San Jose Estepar, *"New Kinematic Metric for Quantifying Surgical,"* in Information Processing in Computer-Assisted Interventions. IPCAI 2010. Lecture Notes in Computer Science, 2010, pp. 81–90.